

Sesuvioside A from *Gomphrena celosioides* possesses the Dual Anti-gout Actions Via Anti-xanthine Oxidase and Anti-inflammatory Activities

Ngo Van Quang^{1*}, Thanh Thi Thu Thuy¹, Dang Vu Luong¹, Trinh Tat Cuong², Nguyen Xuan Ha³, Nguyen Manh Cuong³, Nguyen Thi Mai Phuong^{4,5*}

¹Institute of Chemistry, Vietnam Academy of Science and Technology, 18 Hoang Quoc Viet Road, Cau Giay, Hanoi, Vietnam.

²Key Laboratory for Enzyme and Protein Technology, VNU University of Science, 334 Nguyen Trai Road, Thanh Xuan, Hanoi, Vietnam.

³Institute of Natural Products Chemistry, Vietnam Academy of Science and Technology, 18 Hoang Quoc Viet Road, Cau Giay, Hanoi, Vietnam.

⁴Graduate University of Science and Technology, Vietnam Academy of Science and Technology, 18 Hoang Quoc Viet Road, Cau Giay, Hanoi, Vietnam.

⁵Institute of Biology, Vietnam Academy of Science and Technology, 18 Hoang Quoc Viet Road, Cau Giay, Hanoi, Vietnam.

***Corresponding author:** Ngo Van Quang, email: nhatquang.ngo@gmail.com; Nguyen Thi Mai Phuong, email: phuongnguyenibt@gmail.com

Received September 6th, 2024; Accepted March 3rd, 2025.

DOI: <http://dx.doi.org/10.29356/jmcs.v69i4.2358>

Abstract. *Gomphrena celosioides* Mart. has been widely used for the treatment of gout in Vietnam. A bio-guided isolation of xanthine oxidase inhibitors revealed that sesuvioside A, the main constituent in the butanol fraction of the aerial parts of *G. celosioides*, is a potential anti-gout compound. The anti-gout activity of sesuvioside A, a main constituent isolated from the butanol fraction for the first time was further extensively investigated using *in vitro* biological assays, including inhibition of xanthine oxidase (XO) activity, nitric oxide (NO), intracellular reactive oxygen species (iROS), pro-inflammatory cytokines productions. The obtained results indicated that sesuvioside A exhibited inhibitory activity against XO and NO production with the IC₅₀ values of 31.6 μ M and 18.3 μ M, respectively. At concentration of 40.0 μ M, the compound significantly reduced iROS level and the production of the pro-inflammatory cytokines TNF- α , IL-6, and IL-8 in the lipopolysaccharide-induced macrophages. A molecular docking study revealed that sesuvioside A strongly binds to the targets XO and p-38 MAPK with the estimated energy of -10.55 kcal/mol and -9.78 kcal/mol, respectively. In conclusion, sesuvioside A from the aerial parts of *G. celosioides* is a new dual anti-gout agent by expressing its inhibitory effects on XO activity and inflammatory targets. The traditional use of *G. celosioides* as a remedy for gout was supported by the findings in this study.

Keywords: *Gomphrena celosioides* Mart; sesuvioside A; xanthine oxidase (XO); anti-inflammatory; anti-gout.

Resumen. La *Gomphrena celosioides* Mart. Es muy usada en Vietnam para el tratamiento de la gota (hiperuricemia). A través de un proceso de aislamiento bio-dirigido de inhibidores de la xantina oxidasa (XO), se identificó que el sesuviósido A, el constituyente principal de la fracción butanólica de las partes aéreas de *G. celosioides*, es un compuesto que mostró actividad farmacológica y es candidato para el desarrollo de medicamentos contra la hiperuricemia. La actividad del sesuviósido A —aislado por primera vez como principal componente de dicha fracción— fue investigada extensamente mediante ensayos biológicos *in vitro*, incluyendo la inhibición de la actividad de la XO, la producción de óxido nítrico (NO), especies reactivas de oxígeno intracelulares (iROS) y citoquinas proinflamatorias. Los resultados obtenidos indicaron que el sesuviósido A

presentó actividad inhibitoria sobre la XO y la producción de NO, con valores de IC₅₀ de 31,6 μ M y 18,3 μ M, respectivamente. A una concentración de 40,0 μ M, el compuesto redujo significativamente los niveles de iROS y la producción de las citoquinas proinflamatorias TNF- α , IL-6 e IL-8 en macrófagos inducidos por lipopolisacáridos. Un estudio de acoplamiento molecular reveló que el sesuviósido A se une fuertemente a los blancos moleculares XO y p38 MAPK, con energías estimadas de -10,55 kcal/mol y -9,78 kcal/mol, respectivamente. En conclusión, el sesuviósido A, aislado de las partes aéreas de *G. celosioides*, representa un nuevo agente anti-gota dual, al ejercer efectos inhibitorios tanto sobre la actividad de la XO como sobre blancos inflamatorios. Los hallazgos de este estudio respaldan el uso tradicional de *G. celosioides* como remedio para la gota.

Palabras clave: *Gomphrena celosioides* Mart.; sesuviósido A; xantina oxidasa (XO); antiinflamatorio; anti-gota (hiperurisemia).

Introduction

Gout is a type of arthritis characterized by sudden and severe pain, redness, and swelling of the joints. This is caused by the accumulation of urate crystals in the joints, ultimately leading to inflammation and severe pain.[1,2] These crystals trigger an immune response, thus inducing the release of inflammatory cytokines such as interferon (IFN)- γ , IL-6, IL-8, IL-10, CCL2, and IL-1 β by assembling and activating the pyrin receptor NOD-like containing 3 (NLRP3), which causes inflammation.[3] The negative effects of urate are primarily due to its ability to trigger the production of intracellular reactive oxygen species (iROS). The activation of the enzymes NADPH oxidase, xanthine oxidase (XO), and nitric oxide synthase results in the production of hydrogen peroxide (H₂O₂), superoxide anion (O₂⁻), and nitric oxide (NO⁻)/proximities (ONOO⁻), respectively, thereby increasing gout-induced joint damage.[4,5] Current conventional medical treatments for gout focus on chemical drugs, such as nonsteroidal anti-inflammatory drugs (NSAIDs) and urate-lowering drugs; however, long-term treatment also leads to unwanted side effects.

Flavones are a group of naturally occurring compounds that are present in various plants and are known for their diverse biological activities. An important pharmacological property of flavones is their ability to inhibit XO.[6] XO is involved in purine metabolism by catalysing the conversion of hypoxanthine to xanthine and uric acid, which can lead to major complications such as gout and kidney stones.[7] Several flavone compounds, including licoisoflavone A, butein, fisetin, diosmetin, luteolin, chrysin, baicalein, and wogonin were found to be the potent XO inhibitors. These flavones exert their inhibitory effects through a variety of mechanisms, including competitive or non-competitive inhibition of the enzyme active site and regulation of XO expression and activity at the gene level. Studies have reported that flavones possessing XO inhibitory activity can effectively reduce serum uric acid levels, thereby showing their potential as therapeutic agents for treating hyperuricemia in gout patients. Furthermore, these compounds exhibit anti-inflammatory and antioxidant properties that may contribute to their overall beneficial effects in gout treatment.[2,6,8] Moreover, flavones have been demonstrated to modulate the activity of various signalling pathways involved in inflammation, often leading to the generation of iROS, which can cause prolonged inflammation and tissue damage. They can exhibit antioxidant activity by scavenging free radicals and inhibiting oxidative stress.[9] These mechanisms collectively contribute to the suppression of inflammatory processes and make flavones potential candidates for the development of novel anti-inflammatory therapies.

Nitric oxide (NO) is a signaling molecule that plays a key role in the pathogenesis of inflammation the joint, gut and lungs. NO is considered as a pro-inflammatory mediator that induces inflammation due to over production in abnormal situations.[10] Therefore, NO inhibitors represent important therapeutic advance in the management of inflammatory diseases. Selective NO biosynthesis inhibitors and synthetic arginine analogues are proved to be used for the treatment of NO⁻ induced inflammation. Nitrit (NO₂⁻), the one electron oxidation product of NO, is a dietary component and is present basally in red blood cells (RBC; 290 nM) and plasma (120 nM).[11] In tissues, nitrite is reduced along a physiological oxygen and pH gradient by different enzymes to mediate responses, such as the modulation of protein expression, regulation of metabolism,[12, 13] and cytoprotection after ischaemia/reperfusion injury.

Gomphrena celosioides Mart belonging to the Amaranthaceae family, is distributed throughout South America, Africa, Asia, Australia and Vietnam.[14] The aerial parts of this plant have been used in folk medicine in many countries for the treatment of rheumatism, urinary tract, kidney stones, and several other diseases, including skin, respiratory, gastro-intestine, arthritis, hyperalgesia, and diuretic.[15–17] Phytochemical studies of the aerial parts have yielded isolation of 20-hydroxyecdysone; 20-hydroxyecdysone-20,22-monoacetone; umbellatoside B; aurantiamide, 3-(4-hydroxyphenyl) methylpropenoate.[18–20] In Vietnam, *G. celosioides* is commonly used as a folk medicinal plant for gout treatment, however its mechanism of actions have not been fully understood.[21]

In this study, to verify the folk uses of *G. celosioides*, sesuvioside A, a major compound, was isolated from the aerial part butanol fraction of *G. celosioides* and the underlying molecular mechanisms of this compound as a dual anti-gout agent were intensively investigated by exploring its inhibitory effects on XO activity and pro-inflammatory cytokines, NO, and iROS formations in LPS-induced RAW 264.7 macrophages. Molecular docking simulations were performed to determine the binding affinity and possible binding mode of the compound to the targets XO and p-38 MAPK enzymes.

Materials and methods

Materials

Gomphrena celosioides Mart. were collected in Nam Dinh Province, Vietnam, in December 2021 and were identified by Dr. Nguyen Quoc Binh, Vietnam National Museum of Nature, Vietnam Academy of Science and Technology (VAST). A voucher (GC04.10/23-24) was deposited at the Institute of Chemistry, Vietnam.

Xanthine, xanthine oxidase (XO), and lipopolysaccharides (LPS) were purchased from Roche Co., Ltd. (Shanghai, China). Other analytical reagents were purchased from Sigma–Aldrich, Singapore. DMEM, and FBS media for cell culture were ordered from Invitrogen (USA). Macrophage RAW 264.7 cells were supplied by Prof. Domenico Delfino, University of Perugia, Italy.

Extraction and isolation

The aerial part dried powder of *G. celosioides* (3.0 kg) was extracted with ethanol at room temperature for 24 hours (3×4 L) using ultrasonication, followed by solvent evaporation under reduced pressure to obtain the crude extract (ND, 265 g). This crude extract was suspended in water and then partitioned with *n*-hexane, ethyl acetate (EtOAc), and *n*-butanol (BuOH). After removal of the solvent in *vacuo*, the BuOH layers gave NDB (86.0 g). The fraction was then chromatographed on a silica gel column (Merck Silica gel 60, 70–230 mesh) with an elution system of chloroform-acetone gradient (8: 3 \rightarrow 8: 7, v/v) to obtain five subfractions: NDB1 (10.5 g), NDB2 (6.5 g), NDB3 (12.0 g), NDB4 (7.5 g), and NDB5 (5.5 g). The NDB4 sub-fraction was separated by column chromatography on silica gel RP-18 (YMC) and eluted with a mobile phase of acetone–water (0.75: 2, v/v) to yield **1** (102 mg). The NDB2 was separated by column chromatography on silica gel, and eluted with chloroform-acetone (6/1, v/v) to yield **2** (35.2 mg). The NDB5 subfraction was further separated by column chromatography on silica gel RP-18 (YMC) and eluted with a mobile phase of acetone–water (2.5: 1, v/v) to yield **3** (14.8 mg), and **4** (16.3 mg). The chemical structure of compounds was identified by 1D- and 2D-NMR and mass spectrometry (MS).

Xanthine oxidase inhibitory activity

XO inhibitory activity of the samples was determined as described by Noro et al. [22] The amount of formed uric acid was measured at 295 nm at 37°C, pH 7.5. Allopurinol was used as a positive control. The reaction mixture contained 100 μ L of sesuvioside A solution, 300 μ L of 50 mM phosphate buffer with pH 7.5, and 100 μ L of XO enzyme solution (0.2 U/mL).

Cell viability

The macrophage cells (RAW264.7) were cultured (3–5 days) in DMEM medium with 2.0 mM L-glutamine, 10.0 mM HEPES, and 1.0 mM sodium pyruvate, and 10 % fetal bovine serum (FBS- GIBCO) at 37 °C in an incubator with a 5 % CO₂. The cell viability was analyzed by an MTT assay. In brief, the cells were

seeded into 96-well plates (1×10^4 cells/mL) and incubated with various concentrations of sesuvioside A (10, 20, 40, 80, and 100 μ M) for 12 hours. Then, the MTT solution of 0.5 mg/mL was added and incubated for another 4 hours. The formed formazan crystals were solubilized in dimethyl sulfoxide (DMSO), and the optical density (OD) was measured at 570 nm by a microplate reader (PowerWave XS model, BioTek Instruments, Inc., Winooski, VT, USA). The untreated cells were used as a control. The viability rate was calculated as a percentage compared to the non-treated control.

Effect on nitric oxide production

The macrophage cells RAW264.7 were cultured (3-5 days) in DMEM medium with 1.0 mM sodium pyruvate, 2.0 mM L-glutamine, 10.0 mM HEPES, and 10 % fetal bovine serum (FBS - GIBCO) at 37 °C in 5 % CO₂. Then, cells were collected and seeded in a 96-well plate at a concentration of 3×10^4 cells/well and continued to grow for 24 hours before treatment with sesuvioside A at different concentrations for 2 hours. After treatment, cells were stimulated with LPS (100 ng/mL) for 24 hours to generate NO. N^G-Methyl-L-arginine acetate (L-NMMA) was used as a positive control. Nitrite (NO₂⁻), an indicator for NO generation, was determined at 540 nm by a microplate reader (BioTek Elx 800). [23] The NO inhibitory production (IC) was calculated using the formula (1):

$$\text{IC\%} = 100 \% - [\text{OD}_{\text{sample}}/\text{OD}_{\text{LPS}}] * 100 \quad (1)$$

Effect on cytokine

The macrophage RAW264.7 cells were cultured in DMEM medium supplemented with 10 % FBS in 96-well microplates at 37 °C with 5 % CO₂ for 12 hours. The cells were then seeded into 6-well plates (3×10^4 cells/well), followed by treatment with sesuvioside A at concentrations of 5.0, 10.0, 20.0, and 40.0 μ M at 37°C for 1 hour, and stimulated with LPS (100 ng/mL) at 37°C for 24 hours. The levels of TNF- α , IL- 6, IL8 and IL-10 in the supernatant were measured using the ELISA kits according to the manufacturer's instructions.

Effect on iROS generation

The iROS were assessed as previously described,[24] in which 2',7'-dichlorofluorescein diacetate (H2DCFDA) is converted to oxidized forms of dichlorofluorescein and 2',7'-fluorescence (DCF) by iROS. RAW264.7 macrophages in DMEM medium supplemented with 10 % FBS were seeded in a 96-well plate with a density of 3×10^4 cells/well. Cells were incubated for 30 min with different concentrations of sesuvioside A. After that, cells were treated with 20 μ M H2DCFDA for 30 min and then incubated with tert-butyl hydroperoxide (tBHP; 200 μ M in PBS containing 1 % FBS) at 37°C for 1 hour. Fluorescence was measured at excitation and emission wavelengths of 535 nm using a fluorescence microscope (ACCU-SCOPE 3012, New York, USA).

Molecular docking

The structures of sesuvioside A and well-known inhibitors were drawn using Marvin JS software, and the geometric optimization of the structures was performed using the MMFF94s force field with OpenBabel software.[25,26] The crystal structures of p38 MAPK involved in inflammation, and XO involved in uric acid formation were downloaded from the RCSB PDB with the PDB ID, 1WBV and 1FIQ, respectively. [27,28] The preparation of protein structures and compounds was carried out similarly to previous studies.[29] Docking simulations between sesuvioside A and anti-gout targets p38 MAPK and XO were conducted using the AutoDock Vina v1.2.3 program.[30] The binding poses with the lowest binding energies for the compound were selected for further in-depth analysis. The docking program was run with an exhaustiveness value of 400 and a grid box size of X: 31.2 Å, Y: 53.0 Å, Z: 99.0 Å for XO and X: 6.2 Å, Y: 14.5 Å, Z: 36.1 for p-38 MAPK. The Discovery Studio Visualizer software was used for visual inspection of the results and graphical representation.[31]

Statistical analysis

The experiments were conducted in triplicate, and the mean values were subsequently calculated. The results are expressed as the means \pm standard deviations, calculated using Microsoft Office Excel 2016. Statistical analysis was carried out using the Student's *t-test*, with $p \leq 0.05$ considered to be significant.

Results and discussion

Isolation of natural compounds from aerial parts of *G. celosioides*

The XO inhibitory activity of three different solvent partition residues (*n*-hexane, EtOAc, and BuOH) of the ethanol extract of the aerial parts of *G. celosioides* was investigated, revealing that the BuOH fraction possessed the highest activity with an IC₅₀ of 58.3 µg/mL (Table S1, Supporting Information (SI)). From this fraction, four compounds (**1–4**) were isolated (Fig. 1) and their chemical structures were determined, including sesuvioside A (**1**), aurantiamide acetate (**2**), eupalitin (**3**), and myricitrin (**4**) by comparison with their NMR and MS spectral (Figures S1, S2, S3, S4, Supporting Information) data from the literature.[32–35] Among the identified compounds, sesuvioside A (compound 1) showed to be a major compound and was isolated from the aerial parts of *G. celosioides* for the first time.

Sesuvioside A (1): ESI-MS *m/z* 637.1 [M-H]⁻, Calcd for C₂₉H₃₄O₁₆, MW: 638; ¹H-NMR (DMSO-*d*₆, 600 MHz) δ_H 6.87 (s, H-8), 8.10 (d, *J* = 8.4 Hz, H-2'/H-6'), 6.88 (d, *J* = 8.4 Hz, H-3'/H-5'), 3.74 (s, 6-OMe), 3.92 (s, 7-OMe), *Galactose*: 5.34 (d, *J* = 7.5 Hz, H-1''), 3.56 (dd, *J* = 9.0, 7.5 Hz, H-2''), 3.40 (dd, *J* = 9.0, 3.0 Hz, H-3''), 3.60 (t, *J* = 3.0 Hz, H-4''), 3.57 (m, H-5''), 3.26 (dd, *J* = 11.4, 5.4 Hz, H_a-6''), and 3.57 (dd, *J* = 11.4, 1.8 Hz, H_b-6''), *Rhamnose*: 4.39 (d, *J* = 1.2 Hz, H-1'''), 3.37 (dd, *J* = 3.0, 1.2 Hz, H-2'''), 3.28 (dd, *J* = 9.0, 3.0 Hz, H-3'''), 3.09 (t, *J* = 9.0 Hz, H-4'''), 3.35 (m, H-5'''), 1.05 (d, *J* = 6.6 Hz, H-6'''); ¹³C-NMR (DMSO-*d*₆, 150 MHz) δ_C 157 (C-2), 133.3 (C-3), 177.8 (C-4), 151.6 (C-5), 131.7 (C-6), 158.7 (C-7), 91.4 (C-8), 151.8 (C-9), 105.3 (C-10), 120.8 (C-1'), 131.1 (d, C-2'/C-6'), 115.1 (d, C-3'/C-5'), 160.1 (C-4'), 60.1 (6-OMe), 56.5 (7-OMe), *Galactose*: 101.8 (C-1''), 71.1 (C-2''), 73.0 (C-3''), 68.1 (C-4''), 73.7 (C-5''), 65.4 (C-6''), *Rhamnose*: 100.1 (C-1'''), 70.4 (C-2'''), 70.6 (C-3'''), 71.9 (C-4'''), 68.3 (C-5'''), 17.9 (C-6''').

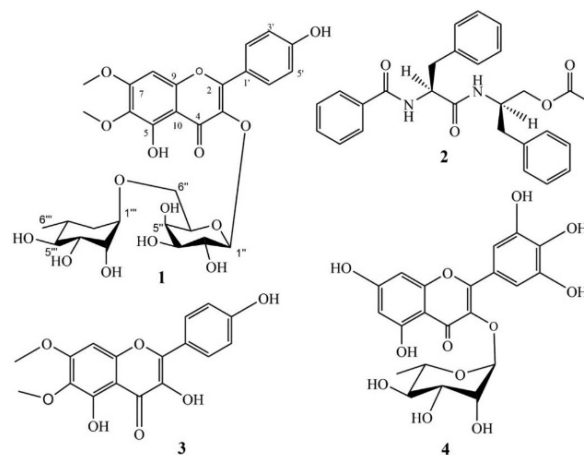


Fig. 1. Chemical structure of sesuvioside A (**1**), aurantiamide acetate (**2**), eupalitin (**3**), and myricitrin (**4**) isolated from the aerial parts of *G. celosioides*

Besides, the results of screening the XO inhibitory activity of the four compounds also indicated that sesuvioside A and aurantiamide acetate were the strongest XO inhibitors with the IC₅₀ values of 31.69 and 28.94 µM, respectively (Table S2, SI). However, cytotoxicity test indicated aurantiamide acetate (compound 2) was significantly cytotoxic toward RAW264.7 cells (Table S3, SI); therefore, sesuvioside A was selected for further study on its anti-inflammatory action mechanism *in vitro*.

Cell cytotoxicity

To select the suitable treatment concentrations for further experiments, sesuvioside A toxicity on RAW 264.7 macrophages was examined. The data in Fig. 2 indicated that sesuvioside A did not affect cell survival at a concentration up to 100.0 µM.

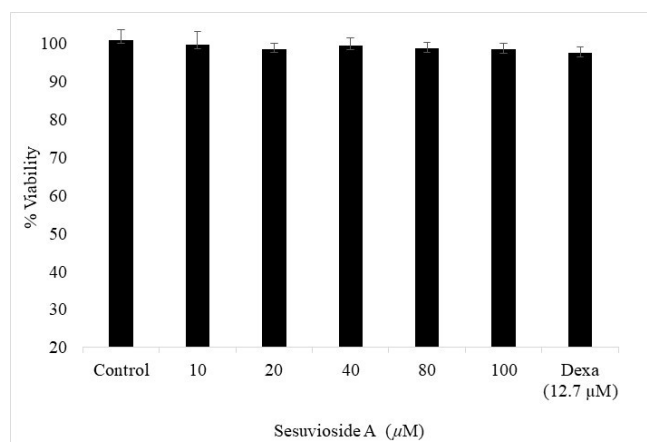


Fig. 2. Cell viability of RAW264.7 cells in the presence of sesuvioside A. Cell viability was determined using the MTT method. The data are expressed as the means \pm SD, ($n = 3$), $p > 0.05$

Xanthine oxidase inhibitory activity

The experimental results (Fig. 3) showed that sesuvioside A exhibited XO inhibitory activity with an IC_{50} value of $31.69 \pm 0.49 \mu M$ which was higher than that of the positive control allopurinol (IC_{50} value of $8.67 \mu M$) (Table S2, SI). Recently, Xu et al. (2023) reported that rutin, another known flavone compound was an XO inhibitor with IC_{50} value of $167.86 \mu M$. Thus, sesuvioside A showed to be a more potent XO inhibitor with an IC_{50} value of 5 folds lower than that of rutin.[36] Li et al. (2022) showed that, owing to glycosylation at the C3 position and increasing steric hindrance, the ability of rutin to inhibit XO was not strong.[37] The two benzopyranone rings (A-B) of rutin stretch the hydrophobic end of XO, whereas the C-ring was inserted into the XO active site and interacts with Phe-1013 and Phe-649 via π - π hydrophobic bonds with a very low affinity, thereby reducing its XO inhibitory activity.[38] For sesuvioside A, the structure of the two methoxy substituents at positions 6 and 7 of the A ring may affect the binding affinity of amino acids in the XO active site. As a result, its inhibitory activity was improved.

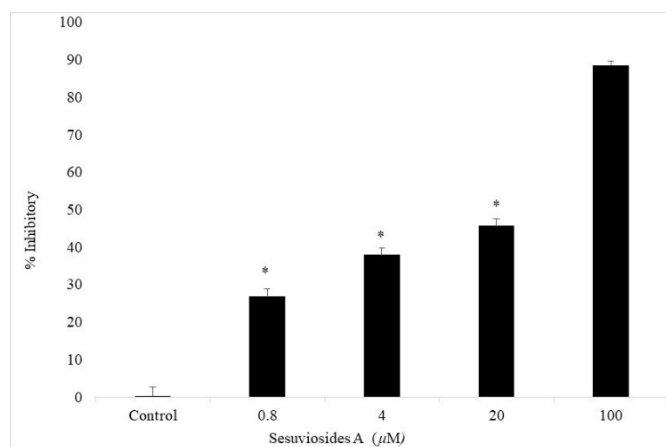


Fig. 3. XO inhibitory effects of sesuvioside A. Data were calculated as a percentage of the untreated sample (control) and are expressed as the means \pm SD ($n = 3$), $p < 0.05$.

Effect on nitric oxide production

Inhibitory activity of sesuvioside A against LPS-induced NO formation in RAW 264.7 cells was evaluated. The data presented in Table 1 indicate that the compound suppressed NO formation with an IC_{50} value of $18.34 \pm 0.15 \mu M$. In contrast, allopurinol (a medication for gout) exhibited no effect (Table S3, SI). The positive control, L-NMMA, possessed an IC_{50} value of $31.93 \pm 1.13 \mu M$. Thus, the NO inhibitory activity of sesuvioside A was markedly better than that of the L-NMMA positive control and even better than the gout medication allopurinol, in terms of NO inhibition. In a previous study, we have reported three compounds umbellatosides B, 20-hydroxyecdysone, and 20-hydroxyecdysone-20,22-monoacetone also isolated from the BuOH fraction of *G. celosioides* possessing the moderate XO and NO inhibitory activities. Of which, umbellatosides B was the most potent inhibitor with IC_{50} values of $33.78 \mu M$ for XO, and $19.55 \mu M$ for NO,[18] nearly the same with sesuvioside A. Thus, our results suggest that there is an anti-gout synergistic effect of multi-compounds rather than a single one. Sesuvioside A and umbellatosides B may be the two significantly contribute to the anti-gout activity of BuOH fraction, as well as of *G. celosioides*.

Table 1. The inhibition of NO production by RAW264.7 macrophages of sesuvioside A.

No	Sesuvioside A			L-NMMA		
	Concentrate (μM)	% cells inhibition of NO	SD	Concentrate ($\mu g/mL$)	% cells inhibition of NO	SD
1	0	0.26	0.05	0	1.65	0.18
2	0.8	16.30	0.02	0.8	9.57	0.29
3	4.0	32.88	0.22	4.0	24.36	0.72
4	20.0	45.20	1.02	20.0	80.73	1.86
5	60.0	61.8	1.06	60.0	92.84	1.08
6	100.0	73.04	1.29	100.0	99.39	1.59
	IC_{50}	$18.34 \pm 0.15 (\mu M)$		IC_{50}	$31.93 \pm 1.13 (\mu M)$	

Note: Samples were incubated with RAW264.7 cells with sesuvioside A for 2 hours before LPS (100 ng/mL) was added and incubated for another 24 hours. The NO-levels were measured at 540 nm and quantitated using the $NaNO_2$ standard curve. L-NMMA was used as a positive control. Data were expressed as means \pm SD (n = 3), $p = 0.017$ (for sesuvioside A), $p = 0.030$ (for L-NMMA).

Effect on cytokine production

The treatment of macrophages with sesuvioside A $\leq 100 \mu M$ for 24 hours did not cause any noticeable effect on cell viability (Fig. 2). Therefore, concentrations ranging from 5.0 to 40.0 μM were selected for evaluation of the inhibitory effects on pro-inflammatory cytokines released by the macrophages. The results presented in Fig. 4 indicate that sesuvioside A 40.0 μM down-regulated TNF- α , IL-6, and IL-8 productions while it had no effect on IL-10 (Fig. 4). It is known that certain inflammatory mediators such as NO, TNF- α , IL-6, and IL-8 are strongly associated with gouty arthritis. [39] The accumulation of these inflammatory mediators in tissues and cells lead to increased damage and consequently promotes severe inflammatory reactions.[40,41] Thus, sesuvioside A suppressed all the pro-inflammatory mediators, thereby reducing inflammation. Our findings agree well with those of quercetin or kaempferol derivatives,[42,43] suggesting the possible applications of sesuvioside A in anti-gouty arthritis.

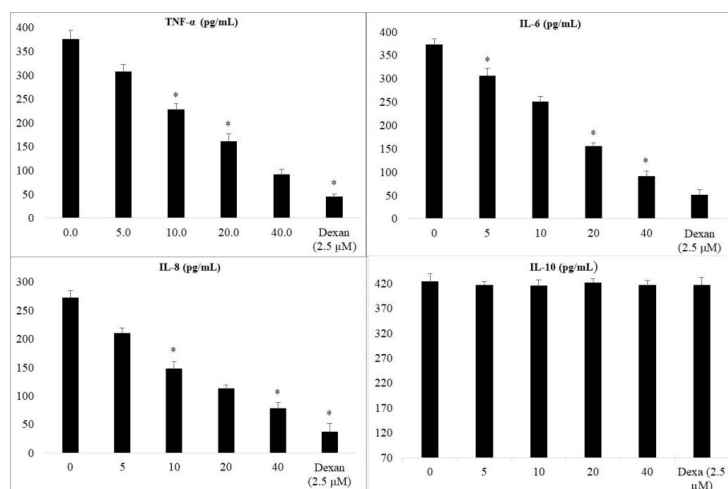


Fig. 4. Effects of sesuvioside A on production of TNF- α , IL-6, IL8, and IL-10 by macrophages. The cells were pretreated with sesuvioside A for 1 hour and then stimulated with LPS (100 ng/mL) for another 24 h. The levels of TNF- α , IL-6, IL-8, and IL-10 were measured using ELISA kits. The data are presented as the means \pm SD ($n = 3$), $p^* < 0.05$.

Effect on iROS generation

iROS is an important signaling factor in LPS-stimulated macrophages. iROS formation in LPS-stimulated macrophages can induce oxidative stress and amplifies the inflammatory response factors.[41] The LPS pre-treated RAW264.7 cell lines can induce large amounts of iROS and therefore, activate various signaling pathways involved in inflammation.[42] In this study, iROS levels generated by LPS induced RAW264.7 macrophages were clearly down-regulated after treatment with sesuvioside A (Fig. 5). At a concentration of 20.0 μ M, the reduction of iROS was not much different compared to that of the control DMSO. However, at a concentration of 40.0 μ M, it was markedly decreased compared to the positive control dexamethasone (Dexa, 2.5 μ M).

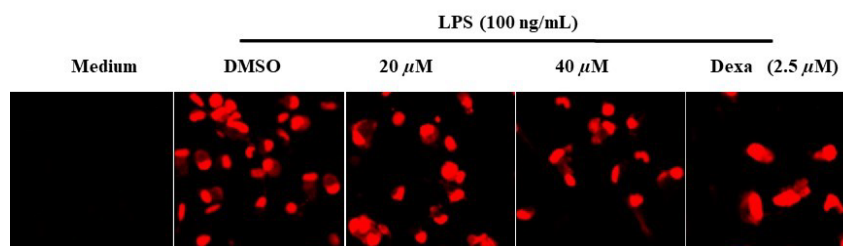


Fig. 5. Effect of sesuvioside A on LPS-induced iROS in RAW264.7 macrophages. The cells were pre-treated with 20.0 μ M and 40.0 μ M sesuvioside A, DMSO, or dexamethasone (Dexa, 2.5 μ M) for 30 min and then treated with LPS (100 ng/ml) for 24 h. The iROS level was detected using a fluorescence microscope (DHE (red) for iROS; scale bar = 200 mm

Molecular docking study

Molecular docking was performed to determine how sesuvioside A binds to possible anti-inflammatory targets such as XO (responsible for uric acid production) and p-38 MAPK (involved in inflammatory signal pathway mitogen activated protein kinase - MAPK). The compound was docked into the active site region of the proteins using a grid box that was determined based on the coordinates of the co-crystallized ligands (Fig. 6).

For XO, it is known that the activation phase of the dehydrogenase to oxidase form by oxidation of sulfhydryl residues or by proteolysis plays an important role in XO activity. [28] The compounds that interfere

with this process by binding to the flavin adenine dinucleotide (FAD) reaction site, the iron/sulfur domain (Fe/S I-II), and/or the molybdopterin center (Mo-pt), may be potent inhibitors of XO. According to the docking results, we found that sesuvioside A mainly interacts with the FAD domain and partly interacts with the Fe/S II binding site of dehydrogenase. Fig. 6(A) clearly shows the function of the di-glycoside moiety to form H-bonding and van der Waals contacts with Glu263, Asp360, and Arg394, which are some of the key residues in the FAD domain. However, the compound could not enter deeply into the domain as the coumarin moiety which exhibited significant hydrophobic interactions at the rim of the pocket (Ile266, Val342) and with residues of the Fe/S II binding site, such as Glu45 and Cys48. This fact could negatively affect the stabilization of sesuvioside A in the complex. In addition, the compound also had some contact with residues of the active loop (pink ribbon from Lys433) that could hinder the dehydrogenase-oxidase transition in XO (Fig. 6). The binding energy of sesuvioside A to XO was estimated to be -10.55 kcal/mol (Table 2).

Table 2. Binding affinity, hydrogen bonding and alkyl interactions of sesuvioside A on proteins XO (PDB ID: 1FIQ) and p38-MAPK (PDB ID: 1WBV).

Compound	Binding affinity (ΔG , kcal/mol)		Hydrogen bonding interactions		Alkyl interactions	
	XO	p-38 MAPK	XO	p-38 MAPK	XO	p-38 MAPK
Sesuvioside A	-10.55	-9.78	Asp360 Arg394 Glu263	Ile147 Gly170 Ala172 His148 Arg189 Arg149 Glu71	Ile266 Val342	Ile 84, Met 78, Arg 67
Allopurinol	-5.7	-	Thr354, Asn261, Val259, Gly260		Glu263	-
3-fluoro-N-1H-indol-5-yl-5-morpholin-4-ylbenzamide	-	-9.765	-	Asp168 Glu71	-	Ile141, Met78, Leu75, Thr106, Lys53, Ile84, Ala51, His148

For p38-MAPK, it is expected that sesuvioside A could strictly bind to p38, which is a key regulator of pro-inflammatory cytokine biosynthesis. It is widely known that p38 is activated through ATP and UTP.[44] Gill *et al.* explored the binding modes of p38 by designing several indolyl derivatives targeting ATP binding sites.[27] They crystallized a hit compound, 3-fluoro-N-1H-indol-5-yl-5-morpholin-4-ylbenzamide, which shows an IC_{50} of 162 μM . Our compound, while showing better activity than 3-fluoro-N-1H-indol-5-yl-5-morpholin-4-ylbenzamide, exhibited a different interaction network with the target compared to the co-crystal ligand. Having di-glycoside structure, sesuvioside A mostly interacts with the hydrophilic residues (His148, Gly170, Ala172, Arg189) and those of the ATP ribose binding region (Asp168). These structure - activity relationships (SARs) suggest the importance of polar moieties (e.g., glycosides) and flexibility of the inhibitors. Only two methoxy groups could form stacking interactions with hydrophobic regions 1 and 2 (Fig. 6(B)). The binding energy of sesuvioside A to p38 was about -9.78 kcal/mol (Table 2). The docking results support a different binding mode of sesuvioside A compared to co-crystal compound, as well as some SARs that may increase the binding ability of p38-MAPK inhibitors toward the ATP binding site. More experimental works are needed to clarify this hypothesis.

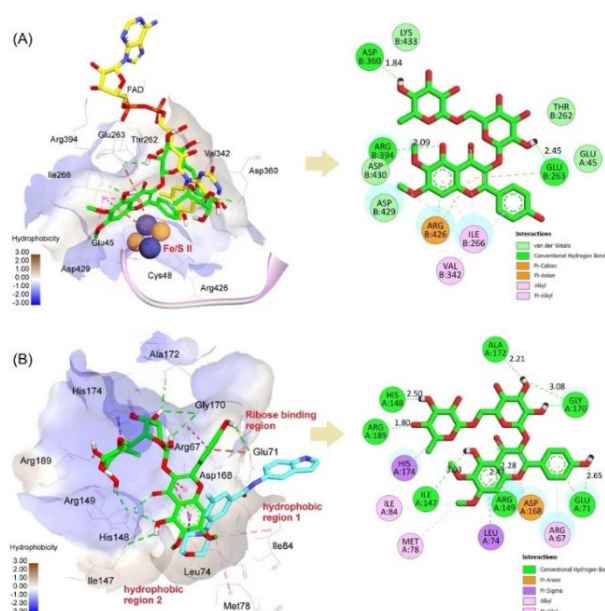


Fig. 6. 3D and 2D interaction diagrams of sesuvioside A (green) against two targets **(A)** XO (PDB ID: 1FIQ) and **(B)** p-38 MAPK (PDB ID: 1WBV). Reference includes two cocrystal-ligands FAD (yellow) and compound 3-fluoro-N-1H-indol-5-yl-5-morpholin-4-ylbenzamide (cyan)

Conclusions

In conclusion, our findings clearly demonstrated that sesuvioside A, a natural compound newly isolated from *G. celosioides*, is a new and promising dual anti-gout agent with multi-target actions, including xanthine oxidase responsible for uric acid synthesis and NO, pro-inflammatory cytokines and iROS formation responsible for inflammation. These results substantiate the potential of *G. celosioides* and sesuvioside A as natural therapeutic agents for the treatment of inflammatory disorders. Nonetheless, further research is essential to fully elucidate their molecular mechanisms of action and to validate their efficacy and safety in animal models. Clinical trials should be followed to examine the optimal dosage, potential drug interactions, and the long-term therapeutic effects in humans.

Acknowledgments

This research was supported by the Vietnam Academy of Science and Technology under grant number VAST04.10/23-24.

References

1. Ragab, G.; Elshahaly, M.; Bardin, T. *J. Adv. Res.* **2017**, *8*, 495–511 DOI: <https://doi.org/10.1016/j.jare.2017.04.008>
2. Huddleston, E. M.; Gaffo, A. L. *Curr. Opin. Pharmacol.* **2022**, *65*, 102241 DOI: <https://doi.org/10.1016/j.coph.2022.102241>
3. Martinon, F.; Pétrilli, V.; Mayor, A.; Tardivel, A.; Tschopp, J. *Nature.* **2006**, *440*, 237–241 DOI: <https://doi.org/10.1038/nature04516>

4. Pouliot, M.; James, M. J.; McColl, S. R.; Naccache, P. H.; Cleland, L. G. *Blood*. **1998**, *91*, 1769–1776.
5. So, A.; Thorens, B. *J. Clin. Invest.* **2010**, *120*, 1791–1799 DOI: <https://doi.org/10.1172/JCI42344>
6. Panche, A. N.; Diwan, A. D.; Chandra, S. R. *J. Nutr. Sci.* **2016**, *5*, e47 DOI: <https://doi.org/10.1017/jns.2016.41>
7. Borges, F.; Fernandes, E.; Roleira, F. *Curr Med Chem.* **2002**, *9*, 195–217 DOI: <https://doi.org/10.2174/0929867023371229>
8. Mierziak, J.; Kostyn, K.; Kulma, A. *Molecules*. **2014**, *19*, 16240–16265 DOI: <https://doi.org/10.3390/molecules191016240>
9. Tian, C.; Liu, X.; Chang, Y.; Wang, R.; Lv, T.; Cui, C.; Liu, M. *S. Afr. J. Bot.* **2021**, *137*, 257–264 DOI: <https://doi.org/10.1016/j.sajb.2020.10.022>
10. Sharma, J. N.; Al-Omran, A.; Parvathy, S. S. *Inflammopharmacol.* **2007**, *15*, 252–259 DOI: <https://doi.org/10.1007/s10787-007-0013-x>
11. Dejam, A.; Hunter, C. J.; Pelletier, M. M.; Hsu, L. L.; Machado, R. F.; Shiva, S.; Power, G. G.; Kelm, M.; Gladwin, M. T.; Schechter, A. N. *Blood*. **2005**, *106*, 734–739 DOI: <https://doi.org/10.1182/blood-2005-02-0567>
12. Larsen, F. J.; Weitzberg, E.; Lundberg, J. O.; Eklom, B. *Free Radical Biol. Med.* **2010**, *48*, 342–347 DOI: <https://doi.org/10.1016/j.freeradbiomed.2009.11.006>
13. Shiva, S.; Huang, Z.; Grubina, R.; Sun, J.; Ringwood, L. A.; MacArthur, P. H.; Xu, X.; Murphy, E.; Darley-Usmar, V. M.; Gladwin, M. T. *Circ. Res.* **2007**, *100*, 654–661 DOI: <https://doi.org/10.1161/01.RES.0000260171.52224.6b>
14. Townsend, C. C. *Springer: Berlin, Heidelberg*. **1993**, 70–91 DOI: https://doi.org/10.1007/978-3-662-02899-5_7
15. Macorini, L. F. B.; Radai, J. A. S.; Maris, R. S.; Silva-Filho, S. E.; Leitao, M. M.; de Andrade, S. F.; Gelves, D. I. A.; Salvador, M. J.; Arena, A. C.; Kassuya, C. A. L. *Evid. Based. Complement. Alternat. Med.* **2020**, *2020*, 4170589 DOI: <https://doi.org/10.1155/2020/4170589>
16. Tarnam, Y. A.; Ilyas, M.; Begum, T. N. *Int. J. Pharma. Res. Rev.* **2014**, *3*, 58–66.
17. de Paula Vasconcelos, P. C.; Spessotto, D. R.; Marinho, J. V.; Salvador, M. J.; Junior, A. G.; Kassuya, C. A. L. *J. Ethnopharmacol.* **2017**, *202*, 85–91 DOI: <https://doi.org/10.1016/j.jep.2017.03.007>
18. Quang, N.; Phuong, N.; Luong, V.; Huyen, N.; Xuan, D.; Thanh, T. *Vietnam J. Chem.* **2024**, *62* DOI: <https://doi.org/10.1002/vjch.202300269>
19. Dosumu, O. O.; Idowu, P. A.; Onocha, P. A.; Ekundayo, O. *EXCLI J.* **2010**, *9*, 173–180.
20. Olutola Dosumu, O.; Onocha, P.; Ekundayo, O.; Ali, M. *Iran. J. Pharm. Res.* **2014**, *13*, 143–147.
21. Hoi, H. *Pharmacogn. J.* **2020**, *12*, 1693–1697 DOI: <https://doi.org/10.5530/pj.2020.12.228>
22. Noro, T.; Oda, Y.; Miyase, T.; Ueno, A.; Fukushima, S. *Chem. Pharm. Bull.* **1983**, *31*, 3984–3987 DOI: <https://doi.org/10.1248/cpb.31.3984>
23. Cheenpracha, S.; Park, E.-J.; Rostama, B.; Pezzuto, J. M.; Chang, L. C. *Mar. Drugs*. **2010**, *8*, 429–437 DOI: <https://doi.org/10.3390/md8030429>
24. Han, Y.-H.; Chen, D.-Q.; Jin, M.-H.; Jin, Y.-H.; Li, J.; Shen, G.-N.; Li, W.-L.; Gong, Y.-X.; Mao, Y.-Y.; Xie, D.-P.; et al. *Appl. Biol. Chem.* **2020**, *63*, 21 DOI: <https://doi.org/10.1186/s13765-020-00504-2>
25. Halgren, T. A. *J. Comput. Chem.* **1999**, *20*, 720–729 DOI: [https://doi.org/10.1002/\(SICI\)1096-987X\(199905\)20:7<720::AID-JCC7>3.0.CO;2-X](https://doi.org/10.1002/(SICI)1096-987X(199905)20:7<720::AID-JCC7>3.0.CO;2-X)
26. O’Boyle, N. M.; Banck, M.; James, C. A.; Morley, C.; Vandermeersch, T.; Hutchison, G. R. *J. Cheminf.* **2011**, *3*, 33 DOI: <https://doi.org/10.1186/1758-2946-3-33>
27. Gill, A. L.; Frederickson, M.; Cleasby, A.; Woodhead, S. J.; Carr, M. G.; Woodhead, A. J.; Walker, M. T.; Congreve, M. S.; Devine, L. A.; Tisi, D.; et al. *J. Med. Chem.* **2005**, *48*, 414–426 DOI: <https://doi.org/10.1021/jm049575n>
28. Enroth, C.; Eger, B. T.; Okamoto, K.; Nishino, T.; Nishino, T.; Pai, E. F. *Proceedings of the National Academy of Sciences*, **2000**, *97*, 10723–10728 DOI: <https://doi.org/10.1073/pnas.97.20.10723>
29. Trott, O.; Olson, A. J. *J. Comput. Chem.* **2010**, *31*, 455–461 DOI: <https://doi.org/10.1002/jcc.21334>

30. Eberhardt, J.; Santos-Martins, D.; Tillack, A. F.; Forli, S. *J. Chem. Inf. Model.* **2021**, *61*, 3891–3898 DOI: <https://doi.org/10.1021/acs.jcim.1c00203>
31. Forli, S.; Huey, R.; Pique, M. E.; Sanner, M. F.; Goodsell, D. S.; Olson, A. J. *Nat. Protoc.* **2016**, *11*, 905–919 DOI: <https://doi.org/10.1038/nprot.2016.051>
32. Disadee, W.; Mahidol, C.; Sahakitpichan, P.; Sitthimonchai, S.; Ruchirawat, S.; Kanchanapoom, T. *Tetrahedron.* **2011**, *67*, 4221–4226 DOI: <https://doi.org/10.1016/j.tet.2011.04.041>
33. Zhou, B.; Yang, Z.; Feng, Q.; Liang, X.; Li, J.; Zanin, M.; Jiang, Z.; Zhong, N. *J. Ethnopharmacol.* **2017**, *199*, 60–67 DOI: <https://doi.org/10.1016/j.jep.2017.01.038>
34. Ghalib, R. M.; Mehdi, S.; Hashim, R.; Sulaiman, O.; Valkonen, A.; Rissanen, K.; Trifunović, S. *J. of Chem. Crystallogr.* **2010**, *40*, 510–513 DOI: <https://doi.org/10.1007/s10870-010-9687-9>
35. Mahmoud, I. I.; Marzouk, M. S.; Moharram, F. A.; El-Gindi, M. R.; Hassan, A. M. *Phytochemistry.* **2001**, *58*, 1239–1244 DOI: [https://doi.org/10.1016/s0031-9422\(01\)00365-x](https://doi.org/10.1016/s0031-9422(01)00365-x)
36. Xue, H.; Xu, M.; Gong, D.; Zhang, G. *Food. Front.* **2023**, *4* DOI: <https://doi.org/10.1002/fft2.287>
37. Li, J.; Gong, Y.; Li, J.; Fan, L. *Food. Chem.* **2022**, *379*, 132100 DOI: <https://doi.org/10.1016/j.foodchem.2022.132100>
38. da Silva, S. L.; da Silva, A.; Honório, K. M.; Marangoni, S.; Toyama, M. H.; da Silva, A. B. F. *J. Mol. Struct. THEOCHEM.* **2004**, *684*, 1–7 DOI: <https://doi.org/10.1016/j.theochem.2004.04.003>
39. Liang, H.; Deng, P.; Ma, Y.-F.; Wu, Y.; Ma, Z.-H.; Zhang, W.; Wu, J.-D.; Qi, Y.-Z.; Pan, X.-Y.; Huang, F.-S.; et al. *Evid. Based. Complement. Alternat. Med.* **2021**, *2021*, 8698232 DOI: <https://doi.org/10.1155/2021/8698232>
40. Turner, M. D.; Nedjai, B.; Hurst, T.; Pennington, D. J. *Biochim. Biophys. Acta.* **2014**, *1843*, 2563–2582 DOI: <https://doi.org/10.1016/j.bbamcr.2014.05.014>
41. Zhang, J.; Li, H.; Wang, W.; Li, H. *Exp. Ther. Med.* **2022**, *23*, 1–8 DOI: <https://doi.org/10.3892/etm.2022.11230>
42. Ying, J.; Zhang, M.; Qiu, X.; Lu, Y. *Biomed. Pharmacother.* **2018**, *103*, 381–390 DOI: <https://doi.org/10.1016/j.biopha.2018.04.088>
43. Yang, L.; He, J. *BMC Complement. Med. Ther.* **2022**, *22*, 55 DOI: <https://doi.org/10.1186/s12906-022-03540-1>
44. Huwiler, A.; Wartmann, M.; van den Bosch, H.; Pfeilschifter, J. *Br. J. Pharmacol.* **2000**, *129*, 612–618 DOI: <https://doi.org/10.1038/sj.bjp.0703077>